Chapter 6
An Assessment of How VDAC Structures Have Impacted Our Understanding of Their Function

Lucie Bergdoll, Michael Grabe, and Jeff Abramson

6.1 Introduction

Mitochondria are the control centers for respiration in all eukaryotic cells producing the vast majority of the universal cellular energy currency, ATP. Efficient exchange of anions, cations, and metabolites between the cytoplasm and the intermembrane space (IMS) of the mitochondria is essential for cellular homeostasis, and this exchange is mediated by the most abundant protein in the outer mitochondrial membrane – the voltage-dependent anion channel (VDAC) (Schein et al. 1976; Rostovtseva and Colombini 1997). Given its role as the primary conduit between the cytoplasm and the mitochondria, VDAC represents an essential cog in the mitochondrial machine's capabilities of modulating mitochondrial activity.

In mammals, there are three VDAC isoforms – VDAC1, VDAC2, and VDAC3 – which have a high degree of sequence similarity (~80%) and wide and overlapping tissue distribution (Fig. 6.1). All isoforms have the ability to transport metabolites and ions (Craigen and Graham 2008); however, they have distinct physiological roles.

L. Bergdoll
Department of Physiology, David Geffen School of Medicine, University of California, Los Angeles, CA, USA

M. Grabe
Cardiovascular Research Institute, Department of Pharmaceutical Chemistry, University of California, San Francisco, CA, USA

J. Abramson (✉)
Department of Physiology, David Geffen School of Medicine, University of California, Los Angeles, CA, USA

Institute for Stem Cell Biology and Regenerative Medicine (inStem), National Centre for Biological Sciences–Tata Institute of Fundamental Research, Bellary Road, Bangalore 560065, Karnataka, India
e-mail: JAbramson@mednet.ucla.edu

T.K. Rostovtseva (ed.), *Molecular Basis for Mitochondrial Signaling*,
Biological and Medical Physics, Biomedical Engineering,
DOI 10.1007/978-3-319-55539-3_6

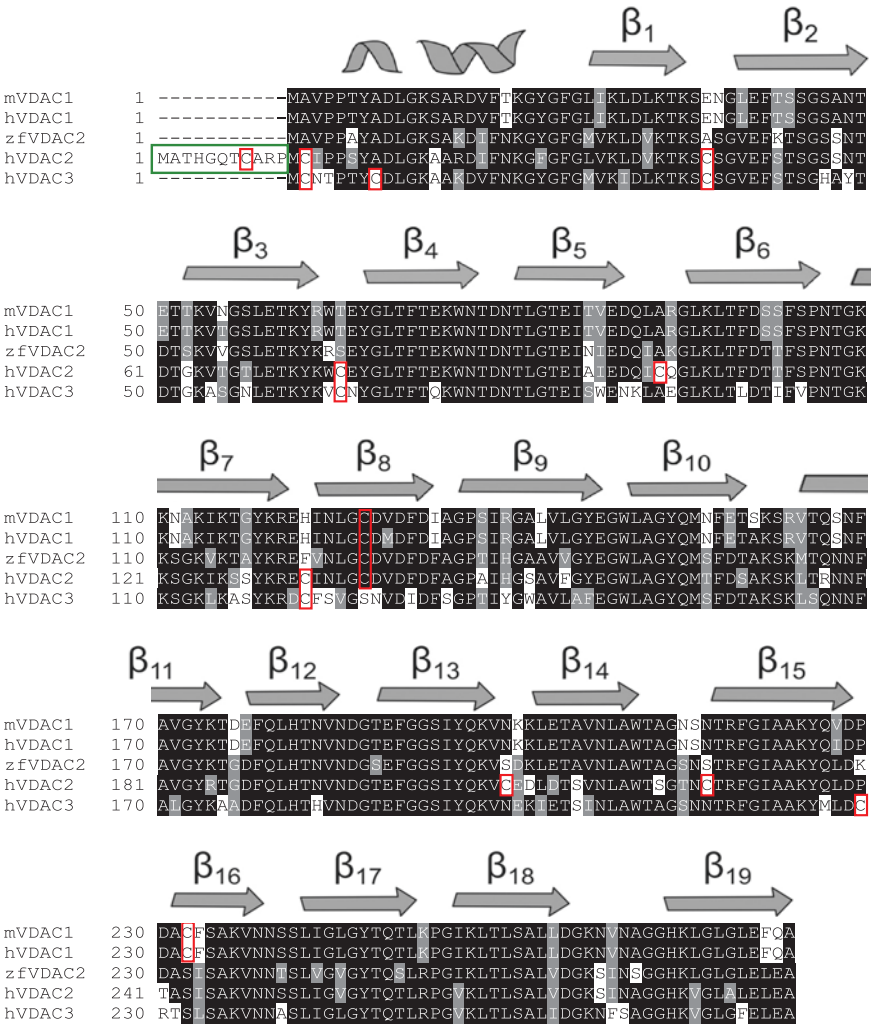

Fig. 6.1 Comparison of VDAC isoforms. Sequence alignment of several VDAC isoforms: mVDAC1 (Q60932), hVDAC1 (P217796), zfVDAC2 (Q8AWD0), hVDAC2 (P45880), and hVDAC3 (Q9Y277). The secondary structure elements are represented on top of the sequence for reference. The cysteine residues are shown in *red boxes*, and the N-terminal extension of 11 amino acids of hVDAC2 is shown in *green*

VDAC1 is the prototypical isoform common to all Eukaryotes and by far the most well characterized (Yamamoto et al. 2006). It is responsible for most of the metabolite transport across the OMM. The human VDAC2 isoform has a unique N-terminal extension of 11 residues and contains 7 additional cysteines compared to hVDAC1 (shown in red in Fig. 6.1). The functional significances of these alterations remain unknown as they have very similar ion and metabolite transport activity. From a

physiological standpoint, VDAC2 has a number of unique properties including favorable calcium transport (Shimizu et al. 2015) and forming complexes with proteins of the Bcl2 family (Roy et al. 2009). VDAC3 is the least abundant isoform, and very little is known about its function. It is noteworthy that while VDAC1 is the most widely expressed isoform, knockout mice lacking VDAC1 display only a mild phenotype. On the contrary, VDAC2 knockout mice are embryonically lethal (Cheng et al. 2003) and knockout mice of VDAC3 lead to male sterility (Sampson et al. 2001).

In 2008, after three decades of biophysical and biochemical characterization, the structure of VDAC1 was resolved by three independent groups using NMR and X-ray crystallography (Bayrhuber et al. 2008; Hiller et al. 2008; Ujwal et al. 2008). Protein structure is a valuable tool for interpreting functional data and driving new experiments to test the proteins' functional properties. Since publishing the structure of murine VDAC1 (Ujwal et al. 2008), its atomic blueprint has been prodded by a large number of cellular, biochemical, and biophysical studies (in excess of 300). In this chapter, we will provide an overview of our current structural knowledge of VDACs and discuss the progress in the field since the structural models have been released. We will also highlight the remaining structural challenges and questions that have yet to be answered.

6.2 The Structure

In 2008, the first structures of VDAC1 were solved by three independent groups: two structures of hVDAC1 – one by NMR (Hiller et al. 2008) and the other using a combination of NMR and X-ray crystallography (Bayrhuber et al. 2008) – and a high-resolution crystal structure of murine VDAC1 at 2.3 Å (mVDAC1) (Ujwal et al. 2008). Murine and human VDAC1 have nearly identical sequences differing by only two conservative amino acid substitutions. The overall structure forms a β-barrel composed of 19 β-strands forming a large pore of 27 Å, with an overall height of 40 Å (Fig. 6.2). As anticipated, the strands are arranged in an antiparallel fashion with the exception of strands 1 and 19, which associate in a parallel manner. The mVDAC1 structure established the position of an N-terminal distorted α-helical segment located approximately halfway down the pore held by strong hydrophobic interactions with β-strand 8 through 18 of the barrel wall. The secondary structure coincides nicely with early circular dichroism studies that predicted a protein composed of both α-helix and β-sheet segments (Shanmugavadivu et al. 2007). These VDAC1 structures, with an odd number of strands, represented a new membrane protein fold since all other known β-barrel membrane proteins are composed of even number of strands (Zeth 2010). In addition, VDAC is one of the two mammalian β-barrel membrane protein structures solved to date with the lymphocyte perforin protein from *Mus musculus* (Law et al. 2010) being the other. By far, the vast majority of β-barrel membrane protein structures are from prokaryotic origin (http://blanco.biomol.uci.edu/mpstruc/).

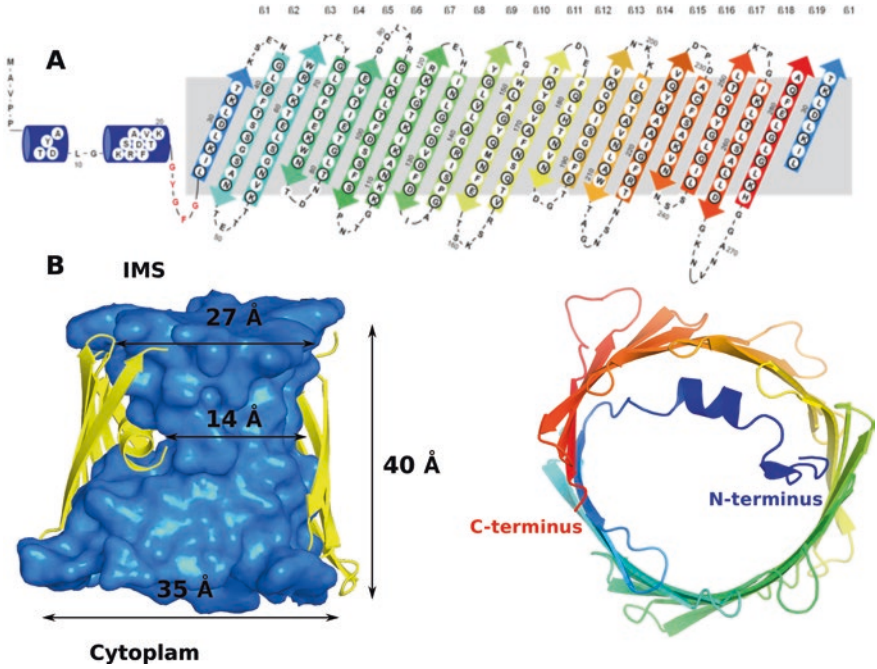

Fig. 6.2 Structural overview of mVDAC1. (**a**) Topology of the primary sequence. (**b**) Cartoon representation of mVDAC1 based on PDB file 3EMN. The left panel is the view from the membrane with β-Strands 3–7 removed for clarity, and the right panel is the top down view from the inter-membrane space (Adapted from Ujwal et al. (2008))

In 2014, a structure of the second isoform from zebrafish (zfVDAC2) was solved at 2.8 Å resolution by X-ray crystallography (Schredelseker et al. 2014). A structural alignment between zfVDAC2 (PDB accession code 4BUM) and mVDAC1 (PDB accession code 3EMN) reveals a small Cα root mean square deviation of 1 Å (between all residues), underscoring their high degree of structural similarity and explaining their similar functional properties (Fig. 6.3). However, it is noteworthy that some of the most striking sequence differences between VDAC1 and VDAC2 discussed previously – namely, the 11 amino acid N-terminal extension and 7 additional cysteines present in mammalian VDAC2 – are not present in zfVDAC2. In this regard, zfVDAC2 has a sequence more similar to VDAC1 than many other VDAC2 subtypes. Nevertheless, a rescue study using zfVDAC2 to rescue the phenotype of VDAC2$^{-/-}$ mouse embryonic fibroblast unambiguously demonstrated that zfVDAC2 had the same functional properties as mammalian VDAC2 (Naghdi et al. 2015). Currently, there are no representative structures from isoform 3 or mammalian isoform 2. The structural difficulties with these later two subtypes are mainly due to difficulties in refolding and obtaining sufficient quantities for structural studies.

The structures of both VDAC1 (mVDAC1 and hVDAC1) and zfVDAC2 isoforms have a glutamate at position 73 (E73), which is facing toward the lipidic milieu (Fig. 6.4). Charged side chains are not frequently observed in such hydrophobic

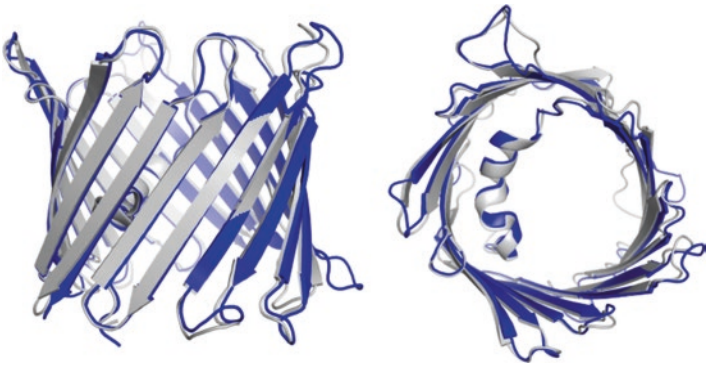

Fig. 6.3 Superimposition of the crystal structures of mVDAC1 (PDB code 3EMN, colored in *gray*) and zfVDAC2 (PDB code 4BUM, colored in *blue*) present a Cα root mean square deviation of 0.98 Å. *Left panel*: view from the membrane; *right panel*: view from the cytosol

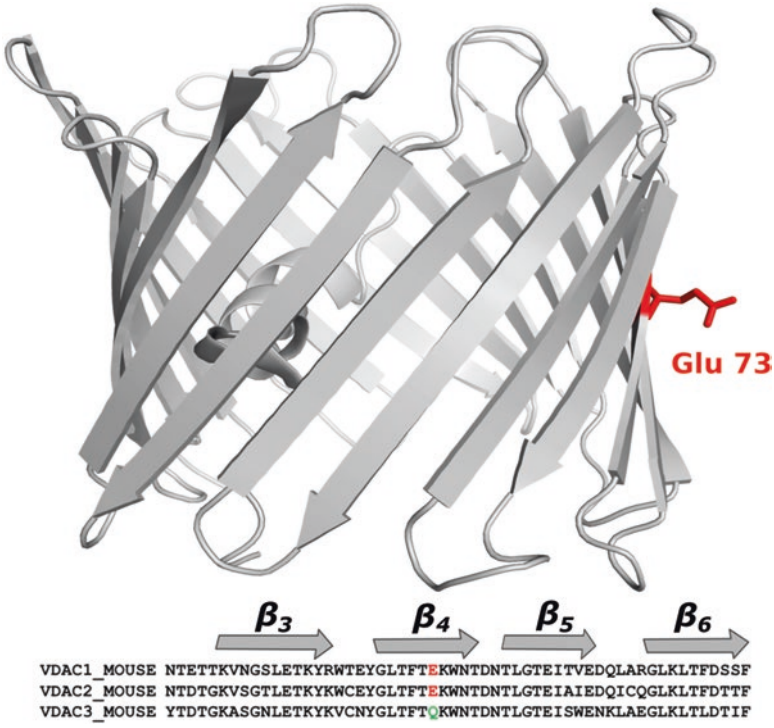

Fig. 6.4 Glutamate 73 is a charged side chain residue pointing toward the membrane. *Bottom*: Sequence alignment of the three mouse VDAC isoforms centered on glutamate 73. VDAC1 and VDAC2 possess a glutamate (*E*) in position 73, whereas VDAC3 possesses a glutamine (*Q*)

environments, but when present they often have a specific functional role. In the case of the transporter LeuT, the basic residue K288 faces the membrane environment, potentially affecting the rate of transition from the outward-facing state to the inward-facing state of the protein (Mondal et al. 2013). Charged residues in the membrane can also serve key functional roles, such as the residue D61 on the rotor of the F_1-F_O ATPase, which binds and releases protons (Valiyaveetil et al. 2002) as they move across the inner mitochondrial membrane imparting rotary torque on the gamma shaft to drive ATP production (Elston et al. 1998)[1]. What role does E73 play in regulating VDAC? Interestingly, cells treated with dicyclohexylcarbodiimide (DCCD), a compound that has been shown to exclusively bind at position E73 in VDAC1, prevent the formation of hexokinase-VDAC1 complex (De Pinto et al. 1993). E73 is also implicated in calcium binding (Ge et al. 2016; Israelson et al. 2007) and calcium-mediated oligomerization (Keinan et al. 2013). The precise functional roles of E73 are not fully understood; however, the third isoform – VDAC3 – has a glutamine at this position (Fig. 6.4) likely leading to isoform-specific function of VDAC3.

Like most high-resolution structures, the structures of VDACs answered many questions regarding their function, but many more questions arose. The most striking one revolved around the physiological relevance of the 2008 structures. It was originally hypothesized, based on the primary sequence, that VDAC would adopt a 19 β-strand fold (Forte et al. 1987); then a second model based on biochemical data suggested a 13 β-strand fold (Colombini 2009). Structure function studies on VDAC were made possible through the development of protocols allowing for the large-scale production of VDAC from inclusion bodies using *E. coli* as an expression host. After in vitro refolding, high yields of pure and homogenous protein, necessary for structure-function studies, could be obtained (Koppel et al. 1998). The 13 β-strand biochemical model, claimed to be the native structure of VDAC in opposition to the solved structure using proteins refolded from inclusion bodies, was strongly refuted by all three structural groups (Hiller et al. 2010). Refolding protein is a commonly used method that does not alter folds as it was proven by many additional studies on membrane proteins prepared from inclusion bodies (such as TOM40 (Kuszak et al. 2015), UCP (Jaburek and Garlid 2003), or Bacteriorhodopsin (Popot et al. 1987)). Furthermore, the structure were solved by solution-NMR in detergent micelles (Hiller et al. 2008; Bayrhuber et al. 2008) as well as by detergent- (Bayrhuber et al. 2008) and lipidic-based crystallization techniques (Ujwal and Abramson 2012; Ujwal et al. 2008) yielding the same 19 β-strand fold. The validity of the structure has been confirmed by numerous studies and methodology including double electron-electron resonance (DEER) (Schredelseker et al. 2014), cross-linking (Teijido et al. 2012; Mertins et al. 2012), and the functional properties of the structure have been confirmed by molecular dynamics simulations and continuum electrostatics calculations – both of which agree well with the known physiological

[1] For a comprehensive list of all residues, on all multipass membrane proteins predicted to be electrostatically destabilizing in the membrane, please see Ref. Marcoline et al. (2015).

ion selectivity values, single-channel conductance values, and ATP permeation rates (Choudhary et al. 2014; Choudhary et al. 2010). To the best of our knowledge, there has not been a single study demonstrating that the 19 β-strand fold is incorrect.

6.3 Conduction Properties and Topology of VDAC

VDAC facilitates the flow of ions and metabolites through the mitochondria. Given its large pore size as revealed in the structures, it is not surprising that it exhibits a high conductance of 0.45–0.58 nS in 0.1 M KCl (Colombini 1989). VDAC's functional activity is routinely monitored electrophysiologically using planar bilayer systems. At low voltage, VDAC adopts an open state allowing ion permeation, with a slight anion selectivity of 1.7–1.9 chloride to potassium ions in a 1.0–0.1 asymmetric gradient (Colombini 1989). A network of charged residues in the pore creating an electric field determines the ion selectivity of VDAC; at high salt concentration the charged residues get shielded and the selectivity decreases (Krammer et al. 2011), the channel is therefore more anion selective at low salt concentration. VDAC is also responsible for metabolite passage, at a flow of 2×10^6 ATP/s under saturating ATP conditions and an estimated 10,000 ATP/s under physiological values (at 1 mM ATP) (Rostovtseva and Colombini 1997). When the voltage is increased, either in the positive or negative direction, the conductance drops to ~0.5 of the open state, corresponding to a closing of the channel, resulting in a bell-shaped current voltage dependence (Fig. 6.5). The closed state displays a negligible metabolite flux but is still permeable to ions and becomes cation selective. There appears to be a single open state; however, the closed configuration is not unique and displays a number of low-conductance states.

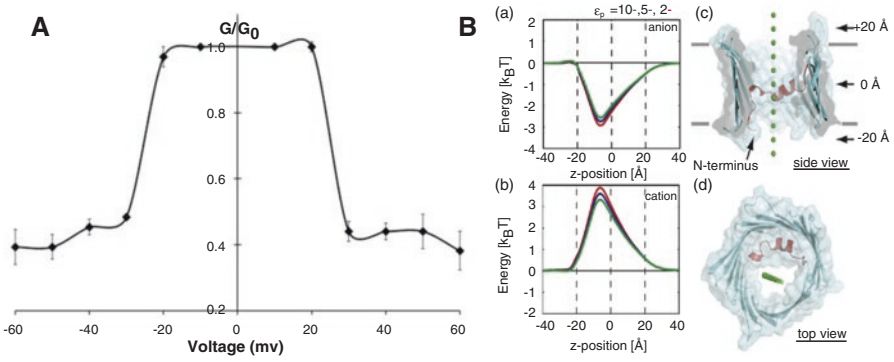

Fig. 6.5 Conduction properties of VDAC. (**A**) Conductance profile of mVDAC1 shows a *bell-shaped curve* with high conductance near 0 mV but reduced conductance at values below −30 mV and above +30 mV (Ujwal et al. 2008). (**B**) The electrostatic energy profile for anions (*a*) and cations (*b*) to move through the channel. The ion pathways traversed in panels *a*, *b* are shown from the side view from the membrane (*c*) and from the cytoplasm (*d*). The negative energy in panel *a* indicates that anions are favored in the pore (Reprinted from Choudhary et al. (2010) with permission from Elsevier)

6.3.1 Computational Studies

The availability of the 3D structure provided a new platform to study VDAC's function. The computational community was essential in validating the structures by relating the physiological properties observed from electrophysiological and biochemical experiments to the 3D architecture. Here we highlight a few of these studies, but a more extensive review on computational technics used to study VDAC can be found in Ref. Noskov et al. (2016).

6.3.1.1 Electrostatic Calculations

The structure revealed a large pore 27 Å in diameter, which is compatible with the high ion flux measured for the open state. This hypothesis was quantitatively probed using a combination of Poisson-Boltzmann (PB) electrostatic calculations and Poisson-Nernst Planck (PNP) theory (Choudhary et al. 2010). The PNP calculations revealed a large single-channel conductance incompatible with the closed state and 1.8–2.3 times higher than the experimental value, which is a typical overestimation for this level of theory when applied to large pores (Im and Roux 2002). However, dramatic improvements of calculated conductance were made possible by the use of long molecular dynamic (MD) simulations (Choudhary et al. 2014), with a calculated value of 0.96 nS in 142 mM NaCl, close to the experimental range of 0.64 to 0.83 nS under these conditions. Interestingly, the presence of ATP in the pore decreases VDAC conductance by 42%, perfectly corroborating the experimental result of 43% obtained on single channels in saturating ATP conditions (Rostovtseva and Bezrukov 1998). Furthermore, the calculations showed a slight preference for anions of 1.75 (Choudhary et al. 2010) in agreement with the experimental anion-to-cation selectivity values of 1.7–1.9 in 1 M KCl (Fig. 6.5). In summary, the electrostatics and MD simulations exploring ion conduction are all *quantitatively* consistent with a high-conductance open state that is selective for anions (Choudhary et al. 2010; Rui et al. 2011; Krammer et al. 2011).

6.3.1.2 Metabolite Permeation

In a recent publication (Choudhary et al. 2014), the permeation pathways of ATP through mVDAC1's pore were deduced using an innovative all-atom Markov state model approach – a first for membrane systems. The structure of VDAC in complex with ATP was also solved (Fig. 6.6) by soaking VDAC crystals in a high concentration of ATP (50 mM). The ATP presented a weak electron density, compatible with a low-affinity site, suggesting a high mobility in the pore. This structure (PDB code 4C69) along with the apo structure (PDB code 3EMN) with ATP placed randomly in solution were used to seed molecular dynamics simulations to investigate ATP permeation through the VDAC pore.

Initially, several multi-microsecond-long simulations carried out using the Anton special-purpose supercomputer at the Pittsburgh Supercomputing Center failed to

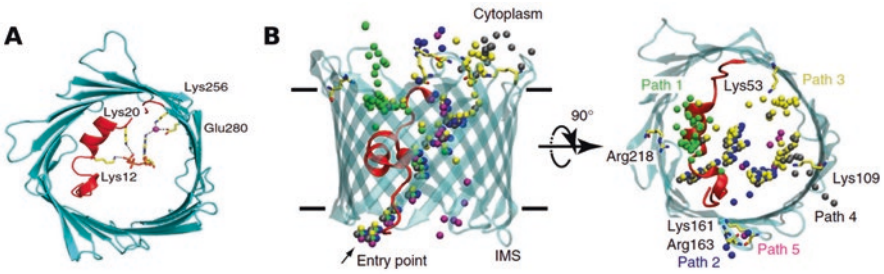

Fig. 6.6 ATP permeation through VDAC. (**A**) Cartoon representation of mVDAC1 in complex with ATP (PDB code 4C69). (**B**) Representation of the five primary pathways of ATP permeation, *dots* represent the γ−phosphate of ATP. ATP permeates the pore via several distinct pathways each lined with basic residues that interact electrostatically with the phosphate group. The *arrow* indicates the common entry point (Reprinted from Choudhary et al. (2014))

reveal ATP permeation. Rather, ATP entered the channel pore from solution where it interacted with the N-terminal helix. As an alternative approach, a Markov state model of ATP permeation was constructed by combining hundreds of short simulations (100–200 ns in length) together to determine how ATP moves through the pore. The simulations showed that ATP moves from one side of the channel to the other in many distinct pathways (top 5 shown in Fig. 6.6B) utilizing the complex network of basic residues facing the pore to "hop" from one position in the pore to the next. The predicted mean first passage time is 32 μs, and the average rate based on this MFPT is ~49,000 ATP/s – a result in excellent agreement with the experimental value of 50,000 ATP/s recorded from *Neurospora crassa* VDAC channels recorded in high ATP concentrations and extrapolated down to 5 mM ATP (Rostovtseva and Colombini 1996). Thus, the ATP flux computed from the MSM again confirms that the crystallographic mVDAC1 structure represents the native open conformation.

6.3.2 VDAC's Orientation in the Membrane

The high-resolution structures did not resolve the debate regarding VDAC's orientation in the membrane, largely due to conflicting biochemical data. This information is essential, since VDAC is a known binding partner for OMM proteins as well as cytosolic and inner membrane space proteins; thus, the correct orientation of the channel is necessary to identify the binding motifs of those various partners. The structure revealed that both N- and C-termini face the same side of the membrane (Ujwal et al. 2008), which was clouded by earlier contradictory studies. Using a combination of antibodies against the N- and C-termini moieties, one study concluded that both extremities where facing the IMS (Stanley et al. 1995). Contrary to this initial claim, a second study found that the N-terminus faces the cytosol and that the C-terminus was buried in the membrane (De Pinto et al. 1991). However, in

2013, this issue was ultimately resolved through studies on VDAC1 in intact cells using a combination of two C-terminal tags on VDAC1 separated by a caspase cleavage site (Tomasello et al. 2013). These researchers conclusively demonstrated that both the N- and C-termini face the IMS of the mitochondria.

6.4 Gating

Since the biochemical and computational studies all indicate that the current VDAC structures represent the open state, the next structural hurdle is to define the closed state(s) and determine how the channel transitions between states. Importantly, it is likely that VDAC channels adopt multiple closed states. There are several known factors that can modulate gating – the transition from open to closed state – including pH (Teijido et al. 2014), voltage (Colombini 1989), lipid composition (Rostovtseva et al. 2006), and salt concentration (Colombini 1989). Although the conformation of the closed state is unknown, the transition from open to closed presumably involves large conformational rearrangements that both hinder the passage of metabolites and alter ion selectivity.

6.4.1 The N-Terminal Helix and Its Influence on Gating

Initial gating hypotheses, developed from visual inspection of the structure, were centered on movements of the N-terminal α-helix. The helix lines the center of the pore causing the diameter to taper from 27 Å at the ends to 14 Å at the center (Fig. 6.2), yet this restriction does not hinder metabolite transport (Choudhary et al. 2014). It was originally postulated that a displacement of the helix away from the wall toward the center of the pore would narrow the cavity even further preventing metabolite permeation (Ujwal et al. 2008; Tornroth-Horsefield and Neutze 2008). Moreover, the helix is rich in charged amino acids and may act as the voltage sensor to facilitate voltage gating, as previously described (Colombini 1989).

This hypothesis was first questioned through the use of continuum electrostatic calculations in which two distinct gating scenarios were evaluated (Choudhary et al. 2010). First, the helix from the mVDAC1 structure was rigidly displaced toward the center of the pore to a position that would dramatically reduce the space available for metabolite permeation (a), and second, the helix was completely removed from the pore (b) leaving only the 19-stranded barrel with a wider pore domain (Fig. 6.7D).

Fig. 6.7 (continued) (**D**) Voltage dependence of gating for mVDAC1 X-ray structure compared to two hypothetical gating motions. In panel (*a*) the N-terminal helix is moved from the wall to the center of the pore. In panel (*b*) the helix is moved out of the pore. The motion in (*a*) produces no voltage-dependent energy change in the system (*blue line* in panel *c*), while the motion in (*b*) produces a modest voltage dependence corresponding to 1.5 gating charges (*red line* in panel *c*) (Reprinted from Choudhary et al. (2010) with permission from Elsevier)

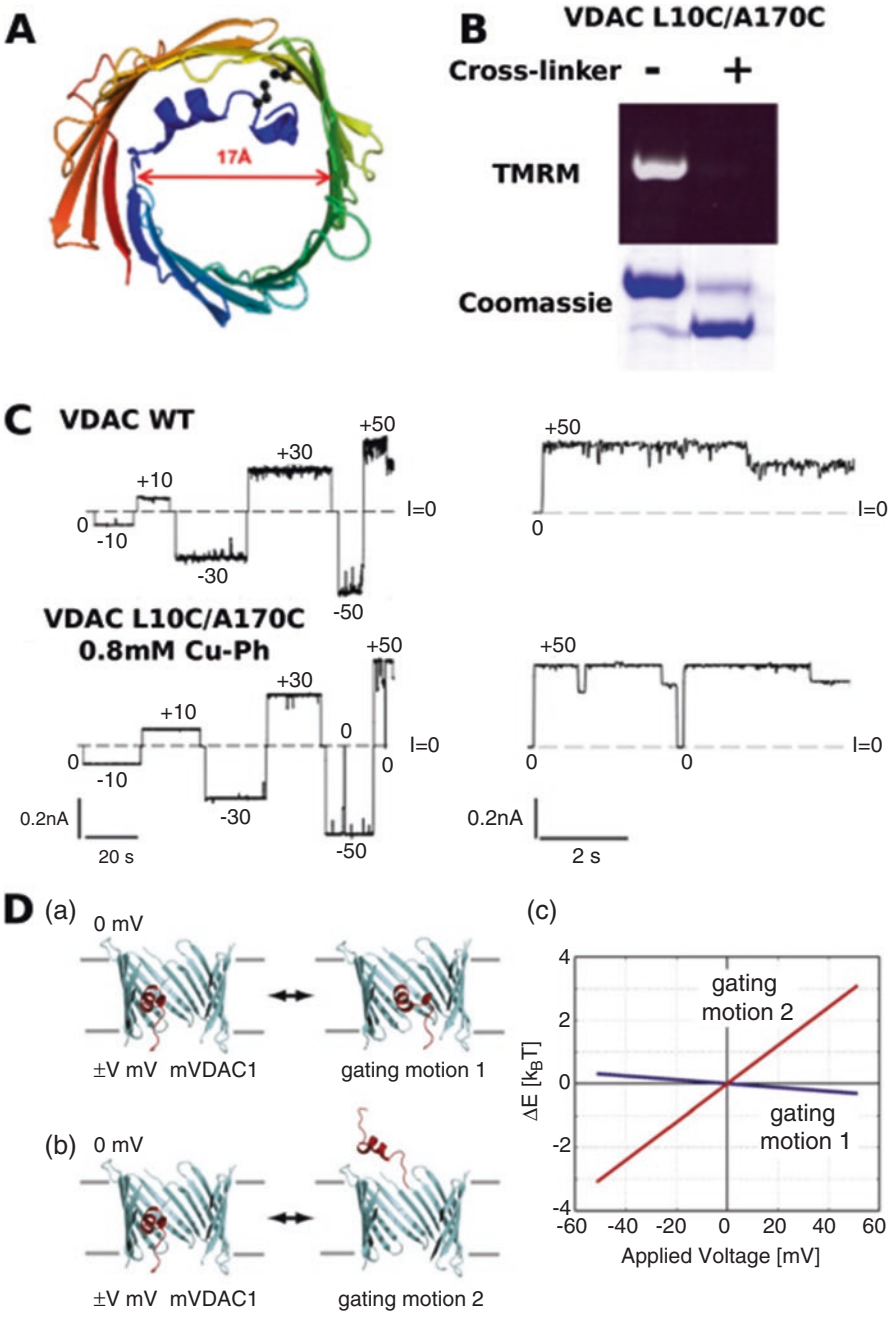

Fig. 6.7 Investigating VDAC's gating mechanism. (**A**) Cartoon representation of mVDAC1 (3EMN) and mutated residues L10C and A170C are displayed in ball and stick form. (**B**) On gel migration of mVDAC 1 L10C/A170C in the absence and presence of cross-linker (CuPh). Cross-linked samples (VDAC L10C/A170C + Cu-Ph) displayed no fluorescence because Cys residues are cross-linked and were not available to react with TMRM. (**C**) Representative records of ion currents through two channels formed by VDAC WT and cross-linked VDAC (Teijido et al. 2012).

Two electrophysiological signatures were used to probe the likelihood that these altered structures had properties of the closed state: (i) the voltage dependence of the gating motion from open to the hypothetical closed state and (ii) the selectivity of the hypothetical closed state. The first quantity indicates how sensitive the gating motion is to changes in the membrane voltage, and the parameter that is used to quantify this sensitivity is the gating charge. This value is the equivalent number of fundamental charge units that pass all the way through the membrane electric field during the gating motion. Channels that are very sensitive to membrane voltage, like voltage-gated potassium channels, exhibit gating charge values between 12 and 14 (Schoppa et al. 1992), and VDAC has a much weaker dependence measured between 2.5 and 4.5 (Colombini 1989; Hiller et al. 2008). As discussed previously, the second physiological property of the closed channel is a slight preference for cations over anions. Analysis of both gating scenarios revealed they failed on both accounts. Both hypothetical closed state models remained anion selective, and the helix hinge motion in the first scenario produce no gating charge at all, while the second helix remove motion only produces a charge of 1.5 – both well below the experimental range of 2.5–4.5 charge units. While these specific transitions are not correct, the calculations could not rule out a more complex movement of the N-terminal helix in combination with other channel conformational changes.

Next, to experimentally test the N-terminal gating model, we employed a combination of electrophysiology and cross-linking experiments (Teijido et al. 2012). The N-terminal α-helix was affixed to the wall of the barrel by creating a covalent bond between Leu-10 and Ala-170 (Fig. 6.7A). Cross-linking was monitored using tetramethylrhodamine (TMRM) (Chaptal et al. 2010) and band-shift on SDS-PAGE (Fig. 6.7B). The effects of the fixation of the helix on gating were monitored in planar lipid bilayers, where the N-terminal cross-linked VDAC formed functional channels of conductance and gating behavior similar to the WT (Fig. 6.7C). This study answered several important questions. First, it was an additional validation of the crystal structure showing that cross-links designed based on the structure could readily be formed in functional studies in the bilayer. Second, the results demonstrated that the gating motion does not involve independent movements of the N-terminal helix with respect to strand 11 on the wall. Surprisingly, another study using similar methodology revealed “asymmetric” gating behavior and preferential selection to a specific closed state (Mertins et al. 2012). Additional experimental studies using a wide array of methodologies coupled with validation through gating charge and selectivity calculations will be required to understand the implication of the N-terminal helix in gating.

6.4.2 A Major Rearrangement of the Barrel

An alternative model of gating is emerging in which the channel elongates in the direction of the principal axis of the N-terminal helix (Teijido et al. 2012; Zachariae et al. 2012). This motion involves VDAC morphing from a cylindrical shape to an

ovular configuration that significantly constricts the pore potentially preventing metabolite passage through steric effects. Consistent with this barrel-constriction hypothesis, MD simulations revealed that VDAC is a flexible barrel that undergoes breathing motions (Villinger et al. 2010). This flexibility is also reflected in the crystallographic b-factors (Ujwal et al. 2008) and the ensemble of structures produced by NMR measurements in solution (Hiller et al. 2008).

Investigating this gating mechanism, Zachariae et al. (2012) carried out MD simulations under applied lateral pressure using a model of mVDAC1 that lacked the N-terminal helix and observed that the channel entered a semi-collapse state inducing an elliptical barrel shape. While this study represents an important step toward understanding channel gating, there are several concerns and unanswered questions: (i) in the presence of the N-terminal helix, this elliptic semi-collapsed state could not be reached, probably because the helix stabilizes the barrel structure, (ii) the elliptic states do not match the cation selectivity observed in the closed state of VDAC, and (iii) the gating charge of this motion was not determined.

From a structural standpoint, investigating VDAC's closed state and gating mechanism is a challenging task due to the difficulty of inducing the closed state in vitro. Indeed, voltage, used to induce gating in lipidic bilayers, cannot be used in solution nor in classical structural biochemistry methods such as NMR or X-ray crystallography. However, other parameters shown to improve gating, such as low pH (Teijido et al. 2014), pressure (Rostovtseva et al. 2006), or salt concentration (Colombini 1989), can be valuable tools to investigate gating.

6.5 Oligomerization

Several lines of evidence suggest that VDAC can adopt various oligomeric states in many different environments ranging from the native mitochondrial membrane to detergent micelles. Clearly this is an area for further investigations as VDAC oligomerization is suggested to play a large role in apoptosis (Keinan et al. 2010; Zalk et al. 2005).

In 2007, prior to the publication of the first high-resolution structures, atomic force microscopy (AFM) studies on the outer mitochondrial membrane of potato tubers (Hoogenboom et al. 2007) and *Saccharomyces cerevisiae* (Goncalves et al. 2007) revealed the organization of VDAC in its native lipidic environment. These studies revealed pores 38 Å wide, which nicely match the diameter values observed in the high-resolution structures. The AFM images showed the presence of monomers, dimers, tetramers, hexamers, and even higher-order oligomers, suggesting that VDAC certainly self-interacts, but the most frequent pore-to-pore distance observed was 53 Å, corresponding to two neighboring pores (Goncalves et al. 2007).

Analysis of crystal packing gave hints to the dimeric organization of VDAC. mVDAC1 crystallizes as an antiparallel dimer (Ujwal et al. 2009), and thus, this interaction is very unlikely to have a physiological relevance, since it is hard to imagine that the channel inserts into the OMM in more than one topological

arrangement. However, both hVDAC1 (Bayrhuber et al. 2008) and zfVDAC2 (Schredelseker et al. 2014) interact as parallel dimers in solution and in the crystal, respectively, with inter-protein interactions occurring across strands, β1, β2, β17, β18, and β19. For both channel isoforms, cross-linking experiments in detergent micelles validated the dimeric association.

6.6 Protein Interactions and Metabolite Binding

6.6.1 Metabolite Binding

VDAC is responsible for metabolite passage between the cytosol and the mitochondria. The most characterized metabolite transported by VDAC is ATP, which can flow through the open state at a rate of two million molecules per second in vitro under saturating ATP concentrations and up to 10,000 molecules/s under physiological conditions (Rostovtseva and Colombini 1996, 1997). With such a high flux, it is not surprising that all reported metabolites binding to VDAC have low affinities, which makes identifying potential binding sites in the channel difficult. A structure of mVDAC1 in complex with ATP was obtained by soaking crystals in a 50 mM ATP solution, revealing a weak binding site for ATP inside the pore, where it associates with basic residues on the N-terminal helix (Fig. 6.6A) (Choudhary et al. 2014). This structure confirms predictions from earlier experiments suggesting that ATP weakly interacts with VDAC's pore (Rostovtseva and Bezrukov 1998; Rostovtseva et al. 2002; Yehezkel et al. 2006). Mass spectrometry was used to reveal two ATP binding site regions – one in the N-terminal helix and another in the region between positions 110–120 of the barrel (numbering in mVDAC1 and hVDAC1) (Yehezkel et al. 2006). The findings from mass spectrometry were later corroborated by the co-crystal structure and molecular dynamic simulations of ATP permeation through the pore, which showed that the phosphate tail of ATP interacts with residues Lys-113 and Lys-115 on β-barrel wall as well as basic residues Lys-12, Arg-15, and Lys-20 on the helix (Choudhary et al. 2014; Noskov et al. 2013).

The NMR structure of hVDAC1 revealed an additional interaction site for the small-molecule NADH on β-strands 17 and 18 implicating 6 residues (Gly-242, Leu-243, Gly-244, Ala-261, Leu-263, Asp-264) (Hiller et al. 2008). However, all those amino acid side chains are facing out of the pore, indicating a binding of the molecule that would be more a regulatory role than for transport. The crystal structure of mVDAC1 clearly indicates that there is not sufficient space to bind a NADH molecule at this specific position. Nonetheless, the described NADH-binding site is located in the vicinity of the flexible region of the N-terminal segment where the helix unwinds and enters β-strand 1, suggesting that binding of NADH in this area could possibly trigger a structural change in this connecting region between the two structural domains of the helix and barrel. In addition to ATP and ADP, a number of glycolysis intermediates like pyruvate and malate must make their way through the OMM into the IMS through VDAC. In total, there is still very little data on metabolite

binding to VDAC, how molecules move through the channel, and how small molecule binding might bias the conformation of the channel. An important future goal is to design experiments to uncover more of these interaction sites, understand how binding impacts the channel structure, and conversely understand how the channel structure aids small-molecule passage into and out of the mitochondria.

6.6.2 VDAC's Interaction with Protein Partners

In addition to being the primary shuttle for ATP and ADP movement across the outer membrane, VDAC is also an essential component of mitochondrial regulation, which it orchestrates through its binding with various protein partners. There are many reports of VDAC binding to other proteins in the OMM, such as the translocator protein (TSPO) (Fan and Papadopoulos 2013), the proteins forming the mitochondrial permeability transition pore (mPTP) (Shoshan-Barmatz et al. 2008), proteins of the inner mitochondrial membrane (IMM) like ANT (Vyssokikh and Brdiczka 2003), as well as cytosolic proteins, such as hexokinase (De Pinto et al. 1993; Shoshan-Barmatz et al. 2015) and tubulin. Tubulin binding to VDAC results in an interaction that impedes metabolite passage (Rostovtseva and Bezrukov 2008), suggesting a powerful way in which cytoplasmic signals could influence energy production by the mitochondria. With the availability of both VDAC and tubulin structures, a hypothetical docking model was generated (Noskov et al. 2013) in which the negatively charged C-terminal tail of tubulin slides into the positively charged pore of VDAC causing occlusion of the pore that would sterically block ATP passage.

VDAC is also regulated by proteins in the Bcl2 family of proteins (Bak, Bax, and tBid) that control cellular apoptosis. During the early stages of apoptosis, caspase activation induces truncation of Bid to form tBid. tBid then relocates to the OMM triggering oligomerization of Bak into homo-oligomers and hetero-oligomers containing Bax and Bak (Wei et al. 2001; Korsmeyer et al. 2000). This oligomerization process leads to the permeabilization of the OMM. VDAC2 is specifically required for Bak import to the outer mitochondrial membrane and tBid-induced apoptosis (Cheng et al. 2003; Roy et al. 2009). In 2015, an elegant study used the structural information from mVDAC1 and zfVDAC2 to design protein chimeras between VDAC1 and VDAC2 to perform a rescue assay in VDAC2$^{-/-}$ fibroblasts (Naghdi et al. 2015). These chimeras identified the structural motif of VDAC2 necessary for Bak and tBid recruitment and induction of apoptosis. This study not only provided further validation that the VDAC1 and VDAC2 structures are biologically relevant, since the chimeras based on them were successful, but also pinpointed two critical residues in VDAC required for Bak recruitment, Thr-168 and Asp-170. Both of these residues are located on the cytoplasmic side of β-strand 10 of VDAC2 positioned in an ideal place to interact with a soluble protein in the cytoplasm. Superposition of the mVDAC1 structure onto zfVDAC2 revealed a binding pocket in VDAC2, positioned on the cytoplasmic side of the membrane (Naghdi et al. 2015).

This site could explain the specificity of VDAC2 for tBid and Bak binding (Naghdi et al. 2015). Interestingly, even though zfVDAC2 differs from mammalian VDAC2 due to its lack of the N-terminal extension and the absence of several cysteines (Fig. 6.1), it is able to recruit Bak and cause apoptosis in mouse embryonic fibroblasts, indicating that zfVDAC2 is a suitable model for mammalian VDAC2.

While valuable information is available both for tubulin and Bak interaction with VDAC, verification of the binding configuration via structural techniques is missing, yet essential for furthering our understanding of the regulation of outer membrane transport and mitochondria-mediated apoptosis.

6.7 Conclusion and Perspectives

During the last 8 years, impressive progress has been made toward understanding VDAC's function. Most of the new data acquired over this time would not have been possible without the availability of a high-resolution 3D structure, yet there are still many challenges ahead.

Going forward, the field must continue to probe the specific physiological roles of all three VDAC isoforms. From a structural and biophysical approach, gating remains a fundamental target: understanding the nature of the closed state and the gating mechanism of VDAC will provide a breakthrough in the understanding of VDAC function and mitochondrial regulation. What does the closed state look like, and how does VDAC transition from an open to a closed conformation? It appears that the closed conformation may not be a stable state, and as such, the use of conventional structural techniques may fail, and we may have to turn to alternative methods that capture dynamic processes. Finally, from a structural standpoint, VDAC complexes are clearly an obtainable goal but require the formation of stable complexes between VDAC and binding partners. Taken together, the regulation of ion and metabolite permeation through VDAC depends on both channel gating and the channel's interaction with protein-binding partners. These various mechanisms likely give rise to a rich set of channel biophysical properties that cannot be described by a simple two-state gating model. As we uncover this new information, we will gain a deeper understanding of VDAC's ability to regulate the mitochondria under a diverse set of physiological conditions.

Acknowledgment This work was supported by the National Institutes of Health Grant R01 GM 089740 (Grabe) and R01GM078844 (Abramson).

References

Bayrhuber M, Meins T, Habeck M, Becker S, Giller K, Villinger S, Vonrhein C, Griesinger C, Zweckstetter M, Zeth K (2008) Structure of the human voltage-dependent anion channel. Proc Natl Acad Sci U S A 105:15370–15375

Chaptal V, Ujwal R, Nie Y, Watanabe A, Kwon S, Abramson J (2010) Fluorescence detection of heavy atom labeling (FD-HAL): a rapid method for identifying covalently modified cysteine residues by phasing atoms. J Struct Biol 171:82–87

Cheng EH, Sheiko TV, Fisher JK, Craigen WJ, Korsmeyer SJ (2003) VDAC2 inhibits BAK activation and mitochondrial apoptosis. Science 301:513–517

Choudhary OP, Ujwal R, Kowallis W, Coalson R, Abramson J, Grabe M (2010) The electrostatics of VDAC: implications for selectivity and gating. J Mol Biol 396:580–592

Choudhary OP, Paz A, Adelman JL, Colletier JP, Abramson J, Grabe M (2014) Structure-guided simulations illuminate the mechanism of ATP transport through VDAC1. Nat Struct Mol Biol 21:626–632

Colombini M (1989) Voltage gating in the mitochondrial channel, VDAC. J Membr Biol 111:103–111

Colombini M (2009) The published 3D structure of the VDAC channel: native or not? Trends Biochem Sci 34:382–389

Craigen WJ, Graham BH (2008) Genetic strategies for dissecting mammalian and Drosophila voltage-dependent anion channel functions. J Bioenerg Biomembr 40:207–212

De Pinto V, Prezioso G, Thinnes F, Link TA, Palmieri F (1991) Peptide-specific antibodies and proteases as probes of the transmembrane topology of the bovine heart mitochondrial porin. Biochemistry 30:10191–10200

De Pinto V, Al Jamal JA, Palmieri F (1993) Location of the dicyclohexylcarbodiimide-reactive glutamate residue in the bovine heart mitochondrial porin. J Biol Chem 268:12977–12982

Elston T, Wang H, Oster G (1998) Energy transduction in ATP synthase. Nature 391:510–513

Fan J, Papadopoulos V (2013) Evolutionary origin of the mitochondrial cholesterol transport machinery reveals a universal mechanism of steroid hormone biosynthesis in animals. PLoS One 8:e76701

Forte M, Guy HR, Mannella CA (1987) Molecular genetics of the VDAC ion channel: structural model and sequence analysis. J Bioenerg Biomembr 19:341–350

Ge L, Villinger S, Mari SA, Giller K, Griesinger C, Becker S, Muller DJ, Zweckstetter M (2016) Molecular plasticity of the human voltage-dependent Anion Channel embedded into a membrane. Structure 24:585–594

Goncalves RP, Buzhynskyy N, Prima V, Sturgis JN, Scheuring S (2007) Supramolecular assembly of VDAC in native mitochondrial outer membranes. J Mol Biol 369:413–418

Hiller S, Garces RG, Malia TJ, Orekhov VY, Colombini M, Wagner G (2008) Solution structure of the integral human membrane protein VDAC-1 in detergent micelles. Science 321:1206–1210

Hiller S, Abramson J, Mannella C, Wagner G, Zeth K (2010) The 3D structures of VDAC represent a native conformation. Trends Biochem Sci 35:514–521

Hoogenboom BW, Suda K, Engel A, Fotiadis D (2007) The supramolecular assemblies of voltage-dependent anion channels in the native membrane. J Mol Biol 370:246–255

Im W, Roux B (2002) Ion permeation and selectivity of OmpF porin: a theoretical study based on molecular dynamics, Brownian dynamics, and continuum electrodiffusion theory. J Mol Biol 322:851–869

Israelson A, Abu-Hamad S, Zaid H, Nahon E, Shoshan-Barmatz V (2007) Localization of the voltage-dependent anion channel-1 Ca2+-binding sites. Cell Calcium 41:235–244

Jaburek M, Garlid KD (2003) Reconstitution of recombinant uncoupling proteins: UCP1, -2, and -3 have similar affinities for ATP and are unaffected by coenzyme Q10. J Biol Chem 278:25825–25831

Keinan N, Tyomkin D, Shoshan-Barmatz V (2010) Oligomerization of the mitochondrial protein voltage-dependent anion channel is coupled to the induction of apoptosis. Mol Cell Biol 30:5698–5709

Keinan N, Pahima H, Ben-Hail D, Shoshan-Barmatz V (2013) The role of calcium in VDAC1 oligomerization and mitochondria-mediated apoptosis. Biochim Biophys Acta 1833: 1745–1754

Koppel DA, Kinnally KW, Masters P, Forte M, Blachly-Dyson E, Mannella CA (1998) Bacterial expression and characterization of the mitochondrial outer membrane channel. Effects of n-terminal modifications. J Biol Chem 273:13794–13800

Korsmeyer SJ, Wei MC, Saito M, Weiler S, Oh KJ, Schlesinger PH (2000) Pro-apoptotic cascade activates BID, which oligomerizes BAK or BAX into pores that result in the release of cytochrome c. Cell Death Differ 7:1166–1173

Krammer EM, Homble F, Prevost M (2011) Concentration dependent ion selectivity in VDAC: a molecular dynamics simulation study. PLoS One 6:e27994

Kuszak AJ, Jacobs D, Gurnev PA, Shiota T, Louis JM, Lithgow T, Bezrukov SM, Rostovtseva TK, Buchanan SK (2015) Evidence of distinct channel conformations and substrate binding affinities for the mitochondrial outer membrane protein translocase pore Tom40. J Biol Chem 290:26204–26217

Law RH, Lukoyanova N, Voskoboinik I, Caradoc-Davies TT, Baran K, Dunstone MA, D'Angelo ME, Orlova EV, Coulibaly F, Verschoor S, Browne KA, Ciccone A, Kuiper MJ, Bird PI, Trapani JA, Saibil HR, Whisstock JC (2010) The structural basis for membrane binding and pore formation by lymphocyte perforin. Nature 468:447–451

Marcoline FV, Bethel N, Guerriero CJ, Brodsky JL, Grabe M (2015) Membrane protein properties revealed through data-rich electrostatics calculations. Structure 23:1526–1537

Mertins B, Psakis G, Grosse W, Back KC, Salisowski A, Reiss P, Koert U, Essen LO (2012) Flexibility of the N-terminal mVDAC1 segment controls the channel's gating behavior. PLoS One 7:e47938

Mondal S, Khelashvili G, Shi L, Weinstein H (2013) The cost of living in the membrane: a case study of hydrophobic mismatch for the multi-segment protein LeuT. Chem Phys Lipids 169:27–38

Naghdi S, Varnai P, Hajnoczky G (2015) Motifs of VDAC2 required for mitochondrial Bak import and tBid-induced apoptosis. Proc Natl Acad Sci U S A 112:E5590–E5599

Noskov SY, Rostovtseva TK, Bezrukov SM (2013) ATP transport through VDAC and the VDAC-tubulin complex probed by equilibrium and nonequilibrium MD simulations. Biochemistry 52:9246–9256

Noskov SY, Rostovtseva TK, Chamberlin AC, Teijido O, Jiang W, Bezrukov SM (2016) Current state of theoretical and experimental studies of the voltage-dependent anion channel (VDAC). Biochim Biophys Acta 1858:1778–1790

Popot JL, Gerchman SE, Engelman DM (1987) Refolding of bacteriorhodopsin in lipid bilayers. A thermodynamically controlled two-stage process. J Mol Biol 198:655–676

Rostovtseva TK, Bezrukov SM (1998) ATP transport through a single mitochondrial channel, VDAC, studied by current fluctuation analysis. Biophys J 74:2365–2373

Rostovtseva TK, Bezrukov SM (2008) VDAC regulation: role of cytosolic proteins and mitochondrial lipids. J Bioenerg Biomembr 40:163–170

Rostovtseva T, Colombini M (1996) ATP flux is controlled by a voltage-gated channel from the mitochondrial outer membrane. J Biol Chem 271:28006–28008

Rostovtseva T, Colombini M (1997) VDAC channels mediate and gate the flow of ATP: implications for the regulation of mitochondrial function. Biophys J 72:1954–1962

Rostovtseva TK, Komarov A, Bezrukov SM, Colombini M (2002) Dynamics of nucleotides in VDAC channels: structure-specific noise generation. Biophys J 82:193–205

Rostovtseva TK, Kazemi N, Weinrich M, Bezrukov SM (2006) Voltage gating of VDAC is regulated by nonlamellar lipids of mitochondrial membranes. J Biol Chem 281:37496–37506

Roy SS, Ehrlich AM, Craigen WJ, Hajnoczky G (2009) VDAC2 is required for truncated BID-induced mitochondrial apoptosis by recruiting BAK to the mitochondria. EMBO Rep 10:1341–1347

Rui H, Lee KI, Pastor RW, Im W (2011) Molecular dynamics studies of ion permeation in VDAC. Biophys J 100:602–610

Sampson MJ, Decker WK, Beaudet AL, Ruitenbeek W, Armstrong D, Hicks MJ, Craigen WJ (2001) Immotile sperm and infertility in mice lacking mitochondrial voltage-dependent anion channel type 3. J Biol Chem 276:39206–39212

Schein SJ, Colombini M, Finkelstein A (1976) Reconstitution in planar lipid bilayers of a voltage-dependent anion-selective channel obtained from paramecium mitochondria. J Membr Biol 30:99–120

Schoppa NE, Mccormack K, Tanouye MA, Sigworth FJ (1992) The size of gating charge in wild-type and mutant Shaker potassium channels. Science 255:1712–1715

Schredelseker J, Paz A, Lopez CJ, Altenbach C, Leung CS, Drexler MK, Chen JN, Hubbell WL, Abramson J (2014) High resolution structure and double electron-electron resonance of the zebrafish voltage-dependent anion channel 2 reveal an oligomeric population. J Biol Chem 289:12566–12577

Shanmugavadivu B, Apell HJ, Meins T, Zeth K, Kleinschmidt JH (2007) Correct folding of the beta-barrel of the human membrane protein VDAC requires a lipid bilayer. J Mol Biol 368:66–78

Shimizu H, Schredelseker J, Huang J, Lu K, Naghdi S, Lu F, Franklin S, Fiji HD, Wang K, Zhu H, Tian C, Lin B, Nakano H, Ehrlich A, Nakai J, Stieg AZ, Gimzewski JK, Nakano A, Goldhaber JI, Vondriska TM, Hajnoczky G, Kwon O, Chen JN (2015) Mitochondrial Ca(2+) uptake by the voltage-dependent anion channel 2 regulates cardiac rhythmicity. Elife 4:e04801

Shoshan-Barmatz V, Keinan N, Zaid H (2008) Uncovering the role of VDAC in the regulation of cell life and death. J Bioenerg Biomembr 40:183–191

Shoshan-Barmatz V, Ben-Hail D, Admoni L, Krelin Y, Tripathi SS (2015) The mitochondrial voltage-dependent anion channel 1 in tumor cells. Biochim Biophys Acta 1848:2547–2575

Stanley S, Dias JA, D'Arcangelis D, Mannella CA (1995) Peptide-specific antibodies as probes of the topography of the voltage-gated channel in the mitochondrial outer membrane of Neurospora crassa. J Biol Chem 270:16694–16700

Teijido O, Ujwal R, Hillerdal CO, Kullman L, Rostovtseva TK, Abramson J (2012) Affixing N-terminal alpha-helix to the wall of the voltage-dependent anion channel does not prevent its voltage gating. J Biol Chem 287:11437–11445

Teijido O, Rappaport SM, Chamberlin A, Noskov SY, Aguilella VM, Rostovtseva TK, Bezrukov SM (2014) Acidification asymmetrically affects voltage-dependent anion channel implicating the involvement of salt bridges. J Biol Chem 289:23670–23682

Tomasello MF, Guarino F, Reina s, Messina A, De Pinto V (2013) The voltage-dependent anion selective channel 1 (VDAC1) topography in the mitochondrial outer membrane as detected in intact cell. PLoS One 8:e81522

Tornroth-Horsefield S, Neutze R (2008) Opening and closing the metabolite gate. Proc Natl Acad Sci U S A 105:19565–19566

Ujwal R, Abramson, J (2012) High-throughput crystallization of membrane proteins using the lipidic bicelle method. J Vis Exp 59:e3383

Ujwal R, Cascio D, Colletier JP, Faham S, Zhang J, Toro L, Ping P, Abramson J (2008) The crystal structure of mouse VDAC1 at 2.3 A resolution reveals mechanistic insights into metabolite gating. Proc Natl Acad Sci U S A 105:17742–17747

Ujwal R, Cascio D, Chaptal V, Ping P, Abramson J (2009) Crystal packing analysis of murine VDAC1 crystals in a lipidic environment reveals novel insights on oligomerization and orientation. Channels (Austin) 3:167–170

Valiyaveetil F, Hermolin J, Fillingame RH (2002) pH dependent inactivation of solubilized F1F0 ATP synthase by dicyclohexylcarbodiimide: pK(a) of detergent unmasked aspartyl-61 in *Escherichia coli* subunit c. Biochim Biophys Acta 1553:296–301

Villinger s, Briones R, Giller K, Zachariae U, Lange A, De Groot BL, Griesinger C, Becker S, Zweckstetter M (2010) Functional dynamics in the voltage-dependent anion channel. Proc Natl Acad Sci U S A 107:22546–22551

Vyssokikh MY, Brdiczka D (2003) The function of complexes between the outer mitochondrial membrane pore (VDAC) and the adenine nucleotide translocase in regulation of energy metabolism and apoptosis. Acta Biochim Pol 50:389–404

Wei MC, Zong WX, Cheng EH, Lindsten T, Panoutsakopoulou V, Ross AJ, Roth KA, Macgregor GR, Thompson CB, Korsmeyer SJ (2001) Proapoptotic BAX and BAK: a requisite gateway to mitochondrial dysfunction and death. Science 292:727–730

Yamamoto T, Yamada A, Watanabe M, Yoshimura Y, Yamazaki N, Yoshimura Y, Yamauchi T, Kataoka M, Nagata T, Terada H, Shinohara Y (2006) VDAC1, having a shorter N-terminus than

VDAC2 but showing the same migration in an SDS-polyacrylamide gel, is the predominant form expressed in mitochondria of various tissues. J Proteome Res 5:3336–3344

Yehezkel G, Hadad N, Zaid H, Sivan S, Shoshan-Barmatz V (2006) Nucleotide-binding sites in the voltage-dependent anion channel: characterization and localization. J Biol Chem 281:5938–5946

Zachariae U, Schneider R, Briones R, Gattin Z, Demers JP, Giller K, Maier E, Zweckstetter M, Griesinger C, Becker S, Benz R, De Groot BL, LANGE A (2012) Beta-barrel mobility underlies closure of the voltage-dependent anion channel. Structure 20:1540–1549

Zalk R, Israelson A, Garty ES, Azoulay-Zohar H, Shoshan-Barmatz V (2005) Oligomeric states of the voltage-dependent anion channel and cytochrome c release from mitochondria. Biochem J 386:73–83

Zeth K (2010) Structure and evolution of mitochondrial outer membrane proteins of beta-barrel topology. Biochim Biophys Acta 1797:1292–1299